Berlin Sfb288 Preprint
US-FT/23-99
hep-th/9912196

Thermodynamic Bethe Ansatz of the Homogeneous Sine-Gordon models

O.A. Castro-Alvaredo[♯], A. Fring[⋆], C. Korff[⋆], J.L. Miramontes[♯]

[♯]*Departamento de Física de Partículas, Facultad de Física*
Universidad de Santiago de Compostela
E-15706 Santiago de Compostela, Spain

[⋆]*Institut für Theoretische Physik, Freie Universität Berlin*
Arnimallee 14, D-14195 Berlin, Germany

Abstract

We apply the thermodynamic Bethe Ansatz to investigate the high energy behaviour of a class of scattering matrices which have recently been proposed to describe the Homogeneous sine-Gordon models related to simply laced Lie algebras. A characteristic feature is that some elements of the suggested S-matrices are not parity invariant and contain resonance shifts which allow for the formation of unstable bound states. From the Lagrangian point of view these models may be viewed as integrable perturbations of WZNW-coset models and in our analysis we recover indeed in the deep ultraviolet regime the effective central charge related to these cosets, supporting therefore the S-matrix proposal. For the $SU(3)_k$-model we present a detailed numerical analysis of the scaling function which exhibits the well known staircase pattern for theories involving resonance parameters, indicating the energy scales of stable and unstable particles. We demonstrate that, as a consequence of the interplay between the mass scale and the resonance parameter, the ultraviolet limit of the HSG-model may be viewed alternatively as a massless ultraviolet-infrared-flow between different conformal cosets. For $k = 2$ we recover as a subsystem the flow between the tricritical Ising and the Ising model.

PACS numbers: 11.10Kk, 11.55.Ds, 05.70.Jk, 05.30.-d, 64.60.Fr, 11.30.Er

Castro@fpaxp1.usc.es
Fring@physik.fu-berlin.de
Korff@physik.fu-berlin.de
Miramont@fpaxp1.usc.es

1 Introduction

The thermodynamic Bethe ansatz (TBA) is established as an important method which serves to investigate "off-shell" properties of 1+1 dimensional quantum field theories. Originally formulated in the context of the non-relativistic Bose gas by Yang and Yang [1], it was extended thereafter by Zamolodchikov [2] to relativistic quantum field theories whose scattering matrices factorize into two-particle ones. The latter property is always guaranteed when the quantum field theory in question is integrable. Provided the S-matrix has been determined in some way, for instance via the bootstrap program [3] or by extrapolating semi-classical results, the TBA allows to calculate the ground state energy of the integrable model on an infinite cylinder whose circumference is identified as compactified space direction. When the circumference is sent to zero the effective central charge of the conformal field theory (CFT) governing the short distance behaviour can be extracted. In the case in which the massive integrable field theory is obtained from a conformal model by adding a perturbative term which breaks the conformal symmetry, the TBA constitutes therefore an important consistency check for the S-matrix.

The main purpose of this manuscript is to apply this technique to a class of scattering matrices which have recently been proposed [4] to describe the Homogeneous sine-Gordon models (HSG) [5, 6] related to simply laced Lie algebras. The latter have been constructed as integrable perturbations of WZNW-coset theories [7] of the form G_k/H, where G is a compact simple Lie group, $H \subset G$ a maximal abelian torus and $k > 1$ an integer called the "level". These models constitute particular deformations of coset-models [7], where the specific choice of the groups ensures that these theories possess a mass gap [8]. The defining action of the HSG-models reads

$$S_{\mathrm{HSG}}[g] = S_{\mathrm{CFT}}[g] + \frac{m^2}{\pi\beta^2} \int d^2x \ \langle \Lambda_+, g(\vec{x})^{-1} \Lambda_- g(\vec{x}) \rangle \quad . \tag{1}$$

Here S_{CFT} denotes the coset action, $\langle\ ,\ \rangle$ the Killing form of G and $g(\vec{x})$ a group valued bosonic scalar field. $\Lambda_\pm$ are arbitrary semi-simple elements of the Cartan subalgebra associated with H, which have to be chosen not orthogonal to any root of G and play the role of continuous vector coupling constants. The latter constraints do not restrict the parameter choice in the quantum case with regard to the proposed S-matrix which makes sense for every choice of $\Lambda_\pm$. They determine the mass ratios of the particle spectrum as well as the behaviour of the model under a parity transformation. The parameters m and $\beta^2 = 1/k + O(1/k^2)$ are the bare mass scale and the coupling constant, respectively. The non-perturbative definition of the theory is achieved by identifying $\langle \Lambda_+, g(\vec{x})^{-1} \Lambda_- g(\vec{x}) \rangle$ with a matrix element of the WZNW-field $g(\vec{x})$ taken in the adjoint representation, which is a spinless primary field of the coset-CFT and in addition exchanging β^2 by $1/k$ and m by the renormalised mass [8]. Some of the conformal data of $S_{\mathrm{CFT}}[g]$, which are in principle extractable from the TBA analysis are the Virasoro central charge c of the coset and the conformal dimensions $\Delta, \bar{\Delta}$ of the perturbing operator in the massless limit

$$c_{G_k} = \frac{k \,\dim G}{k+h} - \ell = \frac{k-1}{k+h} h\ell \,, \qquad\qquad \Delta = \bar{\Delta} = \frac{h}{k+h} \,. \tag{2}$$

Here ℓ denotes the rank of G and h its Coxeter number. Since we have $\Delta < 1$ for all allowed values of k, the perturbation is always relevant in the sense of renormalisation*.

The simplest example of a HSG theory is the complex sine-Gordon model [6, 9] associated with the coset $SU(2)_k/U(1)$. As we will argue below, more complicated HSG theories can be viewed as interacting copies of complex sine-Gordon theories. The classical equations of motion of these models correspond to non-abelian affine Toda equations [5, 10], which are known to be classically integrable and admit soliton solutions. Identifying these solutions by a Noether charge allows for a semi-classical approach to the quantum theory by applying the Bohr-Sommerfeld quantization rule. The integrability on the quantum level was established in [8] by the construction of non-trivial conserved charges, which suggests the factorization of the scattering matrix. Based on the assumption that the semi-classical spectrum is exact, the S-matrix elements have then been determined in [4] by means of the bootstrap program for HSG-models related to simply laced Lie algebras.

The proposed scattering matrix consists partially of ℓ copies of minimal $su(k)$-affine Toda field theories (ATFT) [11], whose mass scales are free parameters. The scattering between solitons belonging to different copies is described by an S-matrix which violates parity [4]. These matrices possess resonance poles and the related resonance parameters which characterize the formation of unstable bound states are up to free choice. In the TBA-analysis these resonances lead to the "staircase patterns" in the scaling function, which have been observed previously for similar models [12]. However, in comparison with the models studied so far, the HSG models are distinguished in two aspects. First they break parity invariance and second some of the resonance poles can be associated directly to unstable particles via a classical Lagrangian.

One of the main outcomes of our TBA-analysis is that the suggested [4] scattering matrix leads indeed to the coset central charge (2), which gives strong support to the proposal.

In addition, we present a detailed numerical analysis for the $SU(3)$-HSG model, but expect that many of our findings for that case are generalizable to other Lie groups. The presence of two parameters, i.e. the mass scale and the resonance parameter allow, similar as for staircase models studied previously, to describe the ultraviolet limit of the HSG-model alternatively as the flow between different conformal field theories in the ultraviolet and infrared regime. We find the following

*We slightly abuse here the notation and use c_{G_k} instead of $c_{G_k/U(1)^\ell}$. Since we always encounter these type of coset in our discussion, we can avoid bulky expressions in this way.

massless flow

$$UV \equiv SU(3)_k/U(1)^2 \leftrightarrow SU(2)_k/U(1) \otimes SU(2)_k/U(1) \equiv IR \; . \tag{3}$$

We also observe the flow $(SU(3)_k/U(1)^2)/(SU(2)_k/U(1)) \rightarrow SU(2)_k/U(1)$ as a subsystem inside the HSG-model. For $k = 2$ this subsystem describes the flow between the tricritical Ising and the Ising model previously studied in [13]. In terms of the HSG-model we obtain the following physical picture: The resonance parameter characterizes the mass scale of the unstable particles. Approaching the extreme ultraviolet regime from the infrared we pass various regions: At first all solitons are too heavy to contribute to the off-critical central charge, then the two copies of the minimal ATFT will set in, leading to the central charge corresponding to IR in (3) and finally the unstable bound states will start to contribute such that we indeed obtain (2) as the ultraviolet central charge of the HSG-model.

The two values of the resonance parameter 0 and ∞ are special, corresponding in the classical theory to a choice of the vector couplings in (1) parallel to each other or orthogonal to a simple root, respectively. In the former case parity is restored on the classical as well as on the TBA-level and the central charge corresponding to UV in (3) is also recovered, whereas in the latter case the two copies of the minimal ATFT are decoupled and unstable bound states may not be produced leading to the central charge IR in (3).

Our manuscript is organized as follows: In section 2 we briefly recall the main features of the two-particle HSG S-matrix elements stating them also newly in form of an integral representation. In particular, we comment on the link between unstable particles and resonance poles as well as on the loss of parity invariance. In section 3 we introduce the TBA equations for a parity violating system and carry out the ultraviolet limit recovering the expected coset central charge. In section 4 we present a detailed study for the $SU(3)_k-$HSG model. We discuss the staircase pattern of the scaling function and illustrate how the UV limit for the HSG-model may be viewed as the UV-IR flow between different conformal models. We extract the ultraviolet central charges of the HSG-models. We study separately the case when parity is restored, derive universal TBA-equations and Y-systems. In section 5 we present explicit examples for the specific values $k = 2, 3, 4, \infty$. Our conclusions are stated in section 6.

2 The homogeneous sine-Gordon S-matrix

We shall now briefly recall the main features of the proposed HSG scattering matrix in a form most suitable for our discussion. Labelling the solitons by two quantum numbers, we take the two-particle scattering matrix between soliton (a, i) and soliton (b, j), with $1 \leq a, b \leq k-1$ and $1 \leq i, j \leq \ell$, as a function of the rapidity difference θ to be of the general form $S_{ab}^{ij}(\theta)$. The particular structure of the conjectured HSG S-matrix makes it suggestive to refer to the lower indices as main quantum numbers and to the upper ones as colour. In [4] it was proposed to describe the scattering of solitons which possess the same colour by the S-matrix of the $\mathbb{Z}_k$-Ising model or equivalently the minimal $su(k)$-ATFT [11]

$$
\begin{aligned}
S_{ab}^{ii}(\theta) &= (a+b)_\theta\,(|a-b|)_\theta \prod_{n=1}^{\min(a,b)-1} (a+b-2n)_\theta^2 && (4)\\
&= \exp \int \frac{dt}{t} 2\cosh\frac{\pi t}{k}\left(2\cosh\frac{\pi t}{k} - I\right)_{ab}^{-1} e^{-it\theta}. && (5)
\end{aligned}
$$

Here we have introduced the abbreviation $(x)_\theta = \sinh\frac{1}{2}(\theta + i\frac{\pi x}{k}) / \sinh\frac{1}{2}(\theta - i\frac{\pi x}{k})$ for the general building blocks and denote the incidence matrix of the $su(k)$-Dynkin diagram by I. We re-wrote the above S-matrix from the block form (4) into a form of an integral representation (5), since the latter is more convenient with respect to the TBA analysis. This calculation may be performed by specializing an analysis in [14, 15] to the particular case at hand. The scattering of solitons with different colour quantum numbers was proposed to be described by

$$
\begin{aligned}
S_{ab}^{ij}(\theta) &= (\eta_{ij})^{ab} \prod_{n=0}^{\min(a,b)-1} (-|a-b|-1-2n)_{\theta+\sigma_{ij}}\,, \qquad K_{ij}^g \neq 0,2 && (6)\\
&= (\eta_{ij})^{ab} \exp - \int \frac{dt}{t}\left(2\cosh\frac{\pi t}{k} - I\right)_{ab}^{-1} e^{-it(\theta+\sigma_{ij})}, \quad K_{ij}^g \neq 0,2\,, && (7)
\end{aligned}
$$

with K^g denoting the Cartan matrix of the simply laced Lie algebra g. Here the $\eta_{ij} = \eta_{ji}^*$ are arbitrary k-th roots of -1 taken to the power a times b and the shifts in the rapidity variables are functions of the vector couplings σ_{ij}, which are anti-symmetric in the colour values $\sigma_{ij} = -\sigma_{ji}$. Due to the fact that these shifts are real, the function $S_{ab}^{ij}(\theta)$ for $i \neq j$ will have poles beyond the imaginary axis such that the parameters σ_{ji} characterize resonance poles. An important feature is that (6) is not parity invariant, where parity is broken by the phase factors η as well as the shifts σ. As a consequence, the usual relations

$$
S_{ab}^{ii}(\theta) = S_{ba}^{ii}(\theta) = S_{ab}^{ii}(-\theta^*)^* \qquad \text{and} \qquad S_{ab}^{ii}(\theta) S_{ab}^{ii}(-\theta) = 1 \tag{8}
$$

satisfied by the parity invariant objects (4), are replaced by

$$
S_{ab}^{ij}(\theta) = S_{ba}^{ji}(-\theta^*)^* \qquad \text{and} \qquad S_{ab}^{ij}(\theta) S_{ba}^{ji}(-\theta) = 1 \tag{9}
$$

for the scattering between solitons with different colour values. Important to note is that the first equality in (8) has no analogue in (9). Thus, instead of being real analytic, as $S_{ab}^{ii}(\theta)$, the parity violation forces Hermitian analyticity of $S_{ab}^{ij}(\theta)$ for

$i \neq j$. Anti-particles are constructed in analogy to the ATFT, that is from the automorphism which leaves the $su(k)$-Dynkin diagram invariant, such that $\overline{(a,i)} = (k-a,i)$. The colour of a particle and its anti-particle is identical. The crossing relation of the S-matrix then reads

$$S^{ij}_{\bar{a}b}(\theta) = S^{ij}_{(k-a)b}(\theta) = S^{ji}_{ba}(i\pi - \theta) \ . \tag{10}$$

For a general and more detailed discussion of these analyticity issues see [16] and references therein.

Analyzing the above S-matrix we have the following picture concerning the formation of bound states: Two solitons with the same colour value may form a bound state of the same colour, whilst solitons of different colour with $K_{ij} \neq 0,2$, say (a,i) and (b,j), may only form an unstable state, say $(\tilde{c},\tilde{k})$ whose lifetime and energy scale are characterized by the parameter σ by means of the Breit-Wigner formula, see e.g. [17], in the form

$$\begin{aligned} (M^{\tilde{k}}_{\tilde{c}})^2 - \frac{(\Gamma^{\tilde{k}}_{\tilde{c}})^2}{4} &= (M^i_a)^2 + (M^j_b)^2 + 2M^i_a M^j_b \cosh\sigma\cos\Theta & (11) \\ M^{\tilde{k}}_{\tilde{c}}\Gamma^{\tilde{k}}_{\tilde{c}} &= 2M^i_a M^j_b \sinh|\sigma|\sin\Theta \ , & (12) \end{aligned}$$

where the resonance pole in $S^{ij}_{ab}(\theta)$ is situated at $\theta_R = \sigma - i\Theta$ and $\Gamma^{\tilde{k}}_{\tilde{c}}$ denotes the decay width of the unstable particle with mass $M^{\tilde{k}}_{\tilde{c}}$. In the case $a = b$ these unstable states can be identified with solitons in the semi-classical limit [4, 24]. When σ becomes zero, (12) shows that the unstable particles become stable, but are still not at the same footing as the other asymptotically stable particles. They become virtual states characterized by poles on the imaginary axis beyond the physical sheet.

How many free parameters do we have in our model? Computing mass shifts from renormalisation, we only accumulate contributions from intermediate states having the same colour as the two scattering solitons. Thus, making use of the well known fact that the masses of the minimal $su(k)$-affine Toda theory all renormalise with an overall factor [18], i.e. for the solitons (a,i) we have that $\delta M^i_a/M^i_a$ equals a constant for fixed colour value i and all possible values of the main quantum number a, we acquire in principle ℓ different mass scales $m_1,\ldots,m_\ell$ in the HSG-model. In addition there are $\ell-1$ independent parameters in the model in form of the possible phase shifts $\sigma_{ij} = -\sigma_{ji}$ for each i,j such that $K^g_{ij} \neq 0,2$. This means overall we have $2\ell-1$ independent parameters in the quantum theory. There is a precise correspondence to the free parameters which one obtains from the classical point of view. In the latter case we have the 2ℓ independent components of $\Lambda_\pm$ at our free disposal. This number is reduced by 1 as a result of the symmetry $\Lambda_+ \to c\Lambda_+$ and $\Lambda_- \to c^{-1}\Lambda_-$ which introduces an additional dependence as may be seen from the explicit expressions for the classical mass ratios and the classical resonance shifts

$$\frac{m_i}{m_j} = \frac{M_a^i}{M_a^j} = \sqrt{\frac{(\alpha_i \cdot \Lambda_+)(\alpha_i \cdot \Lambda_-)}{(\alpha_j \cdot \Lambda_-)(\alpha_j \cdot \Lambda_+)}}, \qquad \sigma_{ij} = \ln \sqrt{\frac{(\alpha_i \cdot \Lambda_+)(\alpha_j \cdot \Lambda_-)}{(\alpha_i \cdot \Lambda_-)(\alpha_j \cdot \Lambda_+)}}. \tag{13}$$

Here the α_i are simple roots.

In comparison with other factorizable scattering matrices involving resonance shifts, studied in the literature so far, the proposed HSG scattering matrices differ in two aspects. First of all, they are not parity invariant and second they allow to associate a concrete Lagrangian description. The latter fact can be used to support the picture outlined for the full quantum field theory by a semi-classical analysis. In [24] the semi-classical mass for the soliton (a, i) was found to be

$$M_a^i = \frac{m_i}{\pi \beta^2} \sin \frac{\pi a}{k} \tag{14}$$

where β is a coupling constant and the m_i are the ℓ different mass scales.

3 TBA with parity violation and resonances

In this section we are going to determine the conformal field theory which governs the UV regime of the quantum field theory associated with the S-matrix elements (4) and (6). According to the defining relation (1) and the discussion of the previous section, we expect to recover the WZNW-coset theory with effective central charge (2) in the extreme ultraviolet limit. It is a well established fact that such high energy limits can be performed by means of the TBA. Since up to now such an analysis has only been carried out for parity invariant S-matrices, a few comments are due to implement parity violation. The starting point in the derivation of the key equations are the Bethe ansatz equations, which are the outcome of dragging one soliton, say of type $A = (a, i)$, along the world line. For the time being we do not need the distinction between the two quantum numbers. On this trip the formal wave-function of A picks up the corresponding S-matrix element as a phase factor when meeting another soliton. Due to the parity violation it matters, whether the soliton is moved clockwise or counter-clockwise along the world line, such that we end up with two different sets of Bethe Ansatz equations

$$e^{iLM_A \sinh\theta_A} \prod_{B \neq A} S_{AB}(\theta_A - \theta_B) = 1 \quad \text{and} \quad e^{-iLM_A \sinh\theta_A} \prod_{B \neq A} S_{BA}(\theta_B - \theta_A) = 1\,, \tag{15}$$

with L denoting the length of the compactified space direction. These two sets of equations are of course not entirely independent and may be obtained from each other by complex conjugation with the help of relation (9). We may carry out the thermodynamic limit of (15) in the usual fashion [2] and obtain the following sets of non-linear integral equations

$$\epsilon_A^+(\theta) + \sum_B \Phi_{AB} * L_B^+(\theta) \;=\; r\, M_A \cosh\theta \qquad (16)$$

$$\epsilon_A^-(\theta) + \sum_B \Phi_{BA} * L_B^-(\theta) \;=\; r\, M_A \cosh\theta\ . \qquad (17)$$

As usual we let the symbol '$*$' denote the rapidity convolution of two functions defined by $f * g(\theta) := \int d\theta'/2\pi\, f(\theta-\theta')g(\theta')$. Here $r = m_1 T^{-1}$ is the inverse temperature times the overall mass scale m_1 of the lightest particle and we also re-defined the masses by $M_a^i \to M_a^i/m_1$ keeping, however, the same notation. As very common in these considerations we also introduced the so-called pseudo-energies $\epsilon_A^+(\theta) = \epsilon_A^-(-\theta)$ and the related functions $L_A^\pm(\theta) = \ln(1 + e^{-\epsilon_A^\pm(\theta)})$. The kernels in the integrals carry the information of the dynamical interaction of the system and are given by

$$\Phi_{AB}(\theta) = \Phi_{BA}(-\theta) \;= -i\frac{d}{d\theta}\ln S_{AB}(\theta)\,. \qquad (18)$$

The statistical interaction is chosen to be of fermionic type. Notice that (17) may be obtained from (16) simply by the parity transformation $\theta \to -\theta$ and the first equality in (18). The main difference of these equations in comparison with the parity invariant case is that we have lost the usual symmetry of the pseudo-energies as a function of the rapidities, such that we have now in general $\epsilon_A^+(\theta) \neq \epsilon_A^-(\theta)$. This symmetry may be recovered by restoring parity.

The scaling function, which can also be interpreted as off-critical Casimir energy, may be computed similar as in the usual way

$$c(r) = \frac{3\,r}{\pi^2}\sum_A M_A \int_0^\infty d\theta\, \cosh\theta\,(L_A^-(\theta) + L_A^+(\theta))\,, \qquad (19)$$

once the equations (16) have been solved for the $\epsilon_A^\pm(\theta)$. Of special interest is the deep UV limit, i.e. $r \to 0$, of this function since then its value coincides with the effective central charge $c_{\text{eff}} = c - 12(\Delta_0 + \bar{\Delta}_0)$ of the conformal model governing the high energy behaviour. Here c is the Virasoro central charge and $\Delta_0, \bar{\Delta}_0$ are the lowest conformal dimensions related to the two chiral sectors of the model. Since the WZNW-coset is unitary, we expect that $\Delta_0, \bar{\Delta}_0 = 0$ and $c_{\text{eff}} = c$. This assumption will turn out to be consistent with the analytical and numerical results.

3.1 Ultraviolet central charge for the HSG model

In this section we follow the usual argumentation of the TBA-analysis which leads to the effective central charge, paying, however, attention to the parity violation.

We will recover indeed the value in (2) as the central charge of the HSG-models. First of all we take the limits $r, \theta \to 0$ of (16) and (17). When we assume that the kernels $\Phi_{AB}(\theta)$ are strongly peaked† at $\theta = 0$ and develop the characteristic plateaus one observes for the scaling models, we can take out the L-functions from the integral in the equations (16), (17) and obtain similar to the usual situation

$$\epsilon_A^{\pm}(0) + \sum_B N_{AB} L_B^{\pm}(0) = 0 \qquad \text{with} \qquad N_{AB} = \frac{1}{2\pi} \int_{-\infty}^{\infty} d\theta \; \Phi_{AB}(\theta) \; . \tag{20}$$

Having the resonance parameter σ present in our theory we may also encounter a situation in which $\Phi_{AB}(\theta)$ is peaked at $\theta = \pm\sigma$. This means in order for (20) to be valid, we have to assume $\epsilon_A^{\pm}(0) = \epsilon_A^{\pm}(\pm\sigma)$ in the limit $r \to 0$ in addition to accommodate that situation. For the last assumption we will not provide a rigorous analytical argument, but will justify it instead for particular cases from the numerical results (see e.g. figure 1). Note that in (20) we have recovered the parity invariance.

For small values of r we may approximate, in analogy to the parity invariant situation, $rM_A \cosh\theta$ by $r/2 M_A \exp\theta$, such that taking the derivative of the relations (16) and (17) thereafter yields

$$\frac{\epsilon_A^{\pm}(\theta)}{d\theta} + \frac{1}{2\pi} \sum_B \int_{-\infty}^{\infty} d\theta' \frac{\Phi_{AB}(\pm\theta \mp \theta')}{1 + \exp(\epsilon_B^{\pm}(\theta'))} \frac{d\epsilon_B^{\pm}(\theta')}{d\theta'} \simeq \frac{r}{2} M_A \exp\theta \quad . \tag{21}$$

The scaling function acquires the form

$$c(r) \simeq \frac{3\,r}{2\pi^2} \sum_A M_A \int_0^{\infty} d\theta \; \exp\theta \, (L_A^-(\theta) + L_A^+(\theta)) \, , \qquad \text{for } r \simeq 0 \tag{22}$$

in this approximation. Replacing in (22) the term $r/2M_A \exp\theta$ by the l.h.s. of (21) a few manipulations lead to

$$\lim_{r\to 0} c(r) \simeq \frac{3}{2\pi^2} \sum_{p=+,-} \sum_A \int_{\epsilon_A^p(0)}^{\epsilon_A^p(\infty)} d\epsilon_A^p \left[\ln(1+\exp(-\epsilon_A^p)) + \frac{\epsilon_A^p}{1+\exp(\epsilon_A^p)} \right] \quad . \tag{23}$$

---

†That this assuption holds for the case at hand is most easily seen by noting that the logarithmic derivative of a basic building block $(x)_\theta$ of the S-matrix reads

$$-i \frac{d}{d\theta} \ln(x)_\theta = -\frac{\sin\left(\frac{\pi}{k}\,x\right)}{\cosh\theta - \cos\left(\frac{\pi}{k}\,x\right)} = -2 \sum_{n=1}^{\infty} \sin\left(\frac{\pi}{k}\,x\right) e^{-n|\theta|} \, .$$

From this we can read off directly the decay properties.

Upon the substitution $y_A^p = 1/(1+\exp(\epsilon_A^p))$ we obtain the well known expression for the effective central charge

$$c_{\rm eff} = \frac{6}{\pi^2} \sum_A \mathcal{L}\left(\frac{1}{1+\exp(\epsilon_A^{\pm}(0))}\right) \ . \tag{24}$$

Here we used the integral representation for Roger's dilogarithm function $\mathcal{L}(x) = 1/2 \int_0^x dy (\ln y/(y-1) - \ln(1-y)/y)$, and the facts that $\epsilon_A^+(0) = \epsilon_A^-(0)$, $y_A^+(\infty) = y_A^-(\infty) = 0$. This means we end up precisely with the same situation as in the parity invariant case: Determining at first the phases of the scattering matrices we have to solve the constant TBA-equation (20) and may compute the effective central charge in terms of Roger's dilogarithm thereafter. Notice that in the ultraviolet limit we have recovered the parity invariance and (24) holds for all finite values of the resonance parameter.

For the case at hand we read off from the integral representation of the scattering matrices

$$N_{ab}^{ij} = \delta_{ij}\delta_{ab} - K_{ij}^{g}\, {(K^{su(k)})^{-1}}_{ab} \ . \tag{25}$$

With N_{ab}^{ij} in the form (25) and the identifications $Q_a^i = \prod_{b=1}^{k-1}(1+\exp(-\epsilon_b^i(0)))^{K^{-1}_{ab}}$ the constant TBA-equations are precisely the equations which occurred before in the context of the restricted solid-on-solid models [19, 20]. It was noted in there that (20) may be solved elegantly in terms of Weyl-characters and the reported effective central charge coincides indeed with the one for the HSG-models (2).

It should be noted that we understand the N-matrix here as defined in (20) and not as the difference between the phases of the S-matrix. In the latter case we encounter contributions from the non-trivial constant phase factors η. Also in that case we may arrive at the same answer by compensating them with a choice of a non-standard statistical interaction as outlined in [22].

We would like to close this section with a comment which links our analysis to structures which may be observed directly inside the conformal field theory. When one carries out a saddle point analysis, see e.g. [21], on a Virasoro character of the general form

$$\chi(q) = \sum_{\vec{m}=0}^{\infty} \frac{q^{\frac{1}{2}\vec{m}(\mathbf{1}-N)\vec{m}^t + \vec{m}\cdot\vec{B}}}{(q)_1 \ldots (q)_{(k-1)\ell}} \ , \tag{26}$$

with $(q)_m = \prod_{k=1}^m (1-q^k)$, one recovers the set of coupled equations as (20) and the corresponding effective central charge is expressible as a sum of Roger's dilogarithms as (24). Note that when we choose $g \equiv A_1$ the HSG-model reduces to the minimal ATFT and (26) reduces to the character formulae in [23]. Thus the equations (20) and (24) constitute an interface between massive and massless theories, since they may be obtained on one hand in the ultraviolet limit from a massive model and on the other hand from a limit inside the conformal field theory. This means we can guess a new form of the coset character, by substituting (25) into (26). However, since the specific form of the vector $\vec{B}$ does not enter in this analysis (it distinguishes the different highest weight representations) more work needs to be done in order to make this more than a mere conjecture. We leave this for future investigations.

4 The SU(3)$_k$-HSG model

We shall now focus our discussion on $G = SU(3)_k$. First of all we need to establish how many free parameters we have at our disposal in this case. According to the discussion in section 2 we can tune the resonance parameter and the mass ratio

$$\sigma := \sigma_{21} = -\sigma_{12} \quad \text{and} \quad m_1/m_2 \ . \tag{27}$$

It will also be useful to exploit a symmetry present in the TBA-equations related to $SU(3)_k$ by noting that the parity transformed equations (17) turn into the equations (16) when we exchange the masses of the different types of solitons. This means the system remains invariant under the simultaneous transformations

$$\theta \to -\theta \qquad \text{and} \qquad m_1/m_2 \to m_2/m_1 \ . \tag{28}$$

For the special case $m_1/m_2 = 1$ we deduce therefore that $\epsilon_a^{(1)}(\theta) = \epsilon_a^{(2)}(-\theta)$, meaning that a parity transformation then amounts to an interchange of the colours. Furthermore, we see from (17) and the defining relation $\sigma = \sigma_{21} = -\sigma_{12}$ that changing the sign of the rapidity variable is equivalent to $\sigma \to -\sigma$. Therefore, we can restrict ourselves to the choice $\sigma \geq 0$ without loss of generality.

4.1 Staircase behaviour of the scaling function

We will now come to the evaluation of the scaling function (19) for finite and small scale parameter r. To do this we have to solve first the TBA equations (16) for the pseudo-energies, which up to now has not been achieved analytically for systems with a non-trivial dynamical interaction due to the non-linear nature of the integral equations. Nonetheless, numerically this problem can be controlled relatively well. In the UV regime for $r \ll 1$ one is in a better position and can set up approximate TBA equations involving formally massless particles[‡] for which various approximation schemes have been developed which depend on the general form of the L-functions. Since the latter is not known a priori, one may justify ones assumptions in retrospect by referring to the numerics. In section 5 we present

[‡]The concept of massless scattering has been introduced originally in [13] as follows: The on-shell energy of a right and left moving particle is given by $E_\pm = M/2e^{\pm\theta}$ which is formally obtained from the on-shell energy of a massive particle $E = m\cosh\theta$ by the replacement $\theta \to \theta \pm \sigma/2$ and taking the limit $m \to 0, \sigma \to \infty$ while keeping the expression $M = me^{\theta+\sigma/2}$ finite. It is these on-shell energies we will encounter in our analysis.

numerical solutions for the equations (16) for various levels k showing that the L-functions develop at most two (three if m_1 and m_2 are very different)plateaus in the range $\ln \frac{r}{2} < \theta < \ln \frac{2}{r}$ and then fall off rapidly (see figure 1). This type of behaviour is similar to the one known from minimal ATFT [2, 29], and we can therefore adopt various arguments presented in that context. The main difficulty we have to deal with here is to find the appropriate "massless" TBA equations accommodating the dependence of the TBA equations on the resonance shifts σ.

We start by separating the kernel (18) into two parts

$$\phi_{ab}(\theta) \;=\; \Phi^{ii}_{ab}(\theta) = \int dt \, \left[\delta_{ab} - 2\cosh\tfrac{\pi t}{k}\left(2\cosh\tfrac{\pi t}{k} - I\right)^{-1}_{ab}\right] e^{-it\theta} \,, \tag{29}$$

$$\psi_{ab}(\theta) \;=\; \Phi^{ij}_{ab}(\theta + \sigma_{ji}) = \int dt \, \left(2\cosh\tfrac{\pi t}{k} - I\right)^{-1}_{ab} e^{-it\theta} \quad , i \neq j \,. \tag{30}$$

Here $\phi_{ab}(\theta)$ is just the TBA kernel of the $su(k)$-minimal ATFT and in the remaining kernels $\psi_{ab}(\theta)$ we have removed the resonance shift. Note that ϕ, ψ do not depend on the colour values i, j and may therefore be dropped all together in the notation. The integral representations for these kernels are obtained easily from the expressions (5) and (7). They are generically valid for all values of the level k. The convolution term in (16) in terms of ϕ, ψ is then re-written as

$$\sum_{j=1}^{\ell}\sum_{b=1}^{k-1} \Phi^{ij}_{ab} * L^j_b(\theta) = \sum_{b=1}^{k-1} \phi_{ab} * L^i_b(\theta) + \sum_{\substack{j=1\\ j\neq i}}^{\ell}\sum_{b=1}^{k-1} \psi_{ab} * L^j_b(\theta - \sigma_{ji}) \,. \tag{31}$$

These equations illustrate that whenever we are in a regime in which the second term in (31) is negligible we are left with ℓ non-interacting copies of the $su(k)$-minimal ATFT.

We will now specialize the discussion on the $su(3)_k$-case for which we can eliminate the dependence on σ in the second convolution term by performing the shifts $\theta \to \theta \pm \sigma/2$ in the TBA equations. In the UV limit $r \to 0$ with $\sigma \gg 1$ the shifted functions can be approximated by the solutions of the following sets of integral equations

$$\varepsilon^{\pm}_a(\theta) + \sum_{b=1}^{k-1} \phi_{ab} * L^{\pm}_b(\theta) + \sum_{b=1}^{k-1} \psi_{ab} * L^{\mp}_b(\theta) \;=\; r' \, M^{\pm}_a \, e^{\pm\theta} \tag{32}$$

$$\hat{\varepsilon}^{\pm}_a(\theta) + \sum_{b=1}^{k-1} \phi_{ab} * \hat{L}^{\pm}_b(\theta) \;=\; r' \, M^{\mp}_a \, e^{\pm\theta} \,, \tag{33}$$

where we have introduced the parameter $r' = r\, e^{\frac{\sigma}{2}}/2$ familiar from the discussion of massless scattering and the masses $M^{+/-}_a = M^{(1)/(2)}_a$. The relationship between the solutions of the massless system (32), (33) and those of the original TBA-equations is given by

$$\epsilon_a^{(1)/(2)}(\theta) = \varepsilon^{+/-}(\theta \mp \sigma/2) \qquad \text{for} \quad \ln(r/2) \ll \pm\theta \ll \ln(r/2)+\sigma \tag{34}$$

$$\epsilon_a^{(1)/(2)}(\theta) = \hat{\varepsilon}^{-/+}(\theta \pm \sigma/2) \qquad \text{for} \quad \pm\,\theta \ll \min[\ln(2/r), \ln(r/2)+\sigma)] \tag{35}$$

where we have assumed $m_1 = m_2$. Similar equations may be written down for the generic case. To derive (35) we have neglected here the convolution terms $(\psi_{ab} * L_b^{(1)})(\theta+\sigma)$ and $(\psi_{ab} * L_b^{(2)})(\theta-\sigma)$ which appear in the TBA-equations for $\epsilon_a^{(2)}(\theta)$ and $\epsilon_a^{(1)}(\theta)$, respectively. This is justified by the following argument: For $|\theta| \gg \ln 2/r$ the free on-shell energy term is dominant in the TBA equations, i.e. $\epsilon_a^i(\theta) \approx r\, M_i^a \cosh\theta$ and the functions $L_a^i(\theta)$ are almost zero. The kernels ψ_{ab} are centered in a region around the origin $\theta = 0$ outside of which they exponentially decrease, see footnote in section 3.1. for this. This means that the convolution terms in question can be neglected safely if $\theta \ll \ln(r/2)+\sigma$ and $\theta \gg \ln(2/r)-\sigma$, respectively. Note that the massless system provides a solution for the whole range of θ for non-vanishing L-function only if the ranges of validity in (34) and (35) overlap, i.e. if $\ln(r/2) \ll \min[\ln(2/r), \ln(r/2)+\sigma]$ which is always true in the limit $r \to 0$ when $\sigma \gg 0$. The solution is uniquely defined in the overlapping region. These observations are confirmed by our numerical analysis below.

The resulting equations (33) are therefore decoupled and we can determine $\hat{L}^+$ and $\hat{L}^-$ individually. In contrast, the equations (32) for $L_a^\pm$ are still coupled to each other due to the presence of the resonance shift. Formally, the on-shell energies for massive particles have been replaced by on-shell energies for massless particles in the sense of [13], such that if we interpret r' as an independent new scale parameter the sets of equations (32) and (33) could be identified as massless TBA systems in their own right.

Introducing then the scaling function associated with the system (32) as

$$c_{\mathrm{o}}(r') = \frac{3\,r'}{\pi^2} \sum_{a=1}^{k-1} \int d\theta \ \left[M_a^+\, e^\theta L_a^+(\theta) + \ M_a^-\ e^{-\theta} L_a^-(\theta)\right] \tag{36}$$

and analogously the scaling function associated with (33) as

$$\hat{c}_{\mathrm{o}}(r') = \frac{3\,r'}{\pi^2} \sum_{a=1}^{k-1} \int d\theta \ \left[M_a^+\, e^\theta \hat{L}_a^+(\theta) + M_a^-\ e^{-\theta} \hat{L}_a^-(\theta)\right] \tag{37}$$

we can express the scaling function (19) of the HSG model in the regime $r \to 0$, $\sigma \gg 1$ approximately by

$$\begin{aligned} c(r,\sigma) &= \frac{3\,r\,e^{\frac{\sigma}{2}}}{2\pi^2} \sum_{i=1,2} \sum_{a=1}^{k-1} M_a^i \int d\theta \ \left[\, e^\theta L_a^i(\theta-\sigma/2) + e^{-\theta} L_a^i(\theta+\sigma/2)\right] \\ &\approx c_{\mathrm{o}}(r') + \hat{c}_{\mathrm{o}}(r') \ . \end{aligned} \tag{38}$$

Thus, we have formally decomposed the massive $SU(3)_k$-HSG model in the UV regime into two massless TBA systems (32) and (33), reducing therefore the problem of calculating the scaling function of the HSG model in the UV limit $r \to 0$ to the problem of evaluating the scaling functions (36) and (37) for the scale parameter r'. The latter depends on the relative size of $\ln(2/r)$ and the resonance shift $\sigma/2$. Keeping now $\sigma \gg 0$ fixed, and letting r vary from finite values to the deep UV regime, i.e. $r = 0$, the scale parameter r' governing the massless TBA systems will pass different regions. For the regime $\ln(2/r) < \sigma/2$ we see that the scaling functions (36) and (37) are evaluated at $r' > 1$, whereas for $\ln(2/r) > \sigma/2$ they are taken at $r' < 1$. Thus, when performing the UV limit of the HSG model the massless TBA systems pass formally from the "infrared" to the "ultraviolet" regime with respect to the parameter r'. We emphasize that the scaling parameter r' has only a formal meaning and that the physical relevant limit we consider is still the UV limit $r \to 0$ of the HSG model. However, proceeding this way has the advantage that we can treat the scaling function of the HSG model by the UV and IR central charges of the systems (32) and (33) as functions of r'

$$c(r,\sigma) \approx c_{\mathrm{o}}(r') + \hat{c}_{\mathrm{o}}(r') \approx \begin{cases} c_{IR} + \hat{c}_{IR}\,, & 0 \ll \ln\frac{2}{r} \ll \frac{\sigma}{2} \\ c_{UV} + \hat{c}_{UV}\,, & \frac{\sigma}{2} \ll \ln\frac{2}{r} \end{cases} . \tag{39}$$

Here we defined the quantities $c_{IR} := \lim_{r'\to\infty} c_{\mathrm{o}}(r')$, $c_{UV} := \lim_{r'\to 0} c_{\mathrm{o}}(r')$ and $\hat{c}_{IR}, \hat{c}_{UV}$ analogously in terms of $\hat{c}_{\mathrm{o}}(r')$.

In the case of $c_{IR} + \hat{c}_{IR} \neq c_{UV} + \hat{c}_{UV}$, we infer from (39) that the scaling function develops at least two plateaus at different heights. A similar phenomenon was previously observed for theories discussed in [12], where infinitely many plateaus occurred which prompted to call them "staircase models". As a difference, however, the TBA equations related to these models do not break parity. In the next subsection we determine the central charges in (39) by means of standard TBA central charge calculation, setting up the so-called constant TBA equations.

4.2 Central charges from constant TBA equations

In this subsection we will perform the limits $r' \to 0$ and $r' \to \infty$ for the massless systems (32) and (33) referring to them formally as "UV-" and "IR-limit", respectively, keeping however in mind that both limits are still linked to the UV limit of the HSG model in the scale parameter r as discussed in the preceding subsection. We commence with the discussion of the "UV limit" $r' \to 0$ for the subsystem (32). We then have three different rapidity regions in which the pseudo-energies are approximately given by

$$\varepsilon_a^{\pm}(\theta) \approx \begin{cases} r' M_a\, e^{\pm\theta}, & \text{for } \pm\theta \gg -\ln r' \\ -\sum_b \phi_{ab} * L_b^{\pm}(\theta) - \sum_b \psi_{ab} * L_b^{\mp}(\theta), & \text{for } \ln r' \ll \theta \ll -\ln r' \\ -\sum_b \phi_{ab} * L_b^{\pm}(\theta), & \text{for } \pm\theta \ll \ln r' \end{cases} . \tag{40}$$

We have only kept here the dominant terms up to exponentially small corrections. We proceed analogously to the discussion as may be found in [2, 29]. We see that in the first region the particles become asymptotically free. For the other two regions the TBA equations can be solved by assuming the L-functions to be constant. Exploiting once more that the TBA kernels are centered at the origin and decay exponentially, we can similar as in section 3.1 take the L-functions outside of the integrals and end up with the sets of equations

$$x_a^{\pm} = \prod_{b=1}^{k-1}(1+x_b^{\pm})^{\hat{N}_{ab}}(1+x_b^{\mp})^{N'_{ab}} \qquad \text{for } \ln r' \ll \theta \ll -\ln r' \tag{41}$$

$$\hat{x}_a = \prod_{b=1}^{k-1}(1+\hat{x}_b)^{\hat{N}_{ab}} \qquad \text{for } \pm\theta \ll \ln r' \tag{42}$$

for the constants $x_a^{\pm} = e^{-\varepsilon_a^{\pm}(0)}$ and $\hat{x}_a = e^{-\varepsilon_a^{\pm}(\mp\infty)}$. The N-matrices can be read off directly from the integral representations (29) and (30)

$$\hat{N} := \frac{1}{2\pi}\int \phi = 1 - 2(K^{su(k)})^{-1} \qquad \text{and} \qquad N' := \frac{1}{2\pi}\int \psi = (K^{su(k)})^{-1} \ . \tag{43}$$

Since the set of equations (42) has already been stated in the context of minimal ATFT and its solutions may be found in [29], we only need to investigate the equations (41). These equations are simplified by the following observation. Sending θ to $-\theta$ the constant L-functions must obey the same constant TBA equation (41) but with the role of L_a^+ and L_a^- interchanged. The difference in the masses m_1, m_2 has no effect as long as $m_1 \sim m_2$ since the on-shell energies are negligible in the central region $\ln r' \ll \theta \ll -\ln r'$. Thus, we deduce $x_a^+ = x_a^- =: x_a$ and (41) reduces to

$$x_a = \prod_{b=1}^{k-1}(1+x_b)^{N_{ab}} \qquad \text{with} \quad N = 1 - (K^{su(k)})^{-1} \ . \tag{44}$$

Remarkably, also these set of equations may be found in the literature in the context of the restricted solid-on-solid models [20]. Specializing some of the general Weyl-character formulae in [20] to the $su(3)_k$-case a straightforward calculation leads to

$$x_a = \frac{\sin\left(\frac{\pi\,(a+1)}{k+3}\right)\sin\left(\frac{\pi\,(a+2)}{k+3}\right)}{\sin\left(\frac{\pi\,a}{k+3}\right)\sin\left(\frac{\pi\,(a+3)}{k+3}\right)} - 1 \quad \text{and} \quad \hat{x}_a = \frac{\sin^2\left(\frac{\pi\,(a+1)}{k+2}\right)}{\sin\left(\frac{\pi\,a}{k+2}\right)\sin\left(\frac{\pi\,(a+2)}{k+2}\right)} - 1 \ . \tag{45}$$

Having determined the solutions of the constant TBA equations (41) and (44) one can proceed via the standard TBA calculations along the lines of [2, 13, 29] and compute the central charges from (36), (37) and express them in terms of Roger's dilogarithm function

$$
\begin{aligned}
c_{UV} &= \lim_{r'\to 0} c_{\rm o}(r') = \frac{6}{\pi^2}\sum_{a=1}^{k-1}\left[2\mathcal{L}\left(\frac{x_a}{1+x_a}\right) - \mathcal{L}\left(\frac{\hat{x}_a}{1+\hat{x}_a}\right)\right] , && (46)\\
\hat{c}_{UV} &= \lim_{r'\to 0} \hat{c}_{\rm o}(r') = \frac{6}{\pi^2}\sum_{a=1}^{k-1}\mathcal{L}\left(\frac{\hat{x}_a}{1+\hat{x}_a}\right) . && (47)
\end{aligned}
$$

Using the non-trivial identities

$$
\frac{6}{\pi^2}\sum_{a=1}^{k-1} L\left(\frac{x_a}{1+x_a}\right) = 3\,\frac{k-1}{k+3} \quad \text{and} \quad \frac{6}{\pi^2}\sum_{a=1}^{k-1} L\left(\frac{\hat{x}_a}{1+\hat{x}_a}\right) = 2\,\frac{k-1}{k+2} \tag{48}
$$

found in [30] and [19], we finally end up with

$$
c_{UV} = \frac{(k-1)\,(4k+6)}{(k+3)\,(k+2)} \qquad \text{and} \qquad \hat{c}_{UV} = 2\,\frac{k-1}{k+2} . \tag{49}
$$

For the reasons mentioned above $\hat{c}_{UV}$ coincides with the effective central charge obtained from $su(k)$ minimal ATFT describing parafermions [7] in the conformal limit. Notice that c_{UV} corresponds to the coset $(SU(3)_k/U(1)^2)/(SU(2)_k/U(1))$.

The discussion of the infrared limit may be carried out completely analogous to the one performed for the UV limit. The only difference is that in case of the system (32) the constant TBA equations (41) drop out because in the central region the free energy terms becomes dominant when $r' \to \infty$. Thus in the infrared regime the central charges of both systems coincide with $\hat{c}_{UV}$,

$$
c_{IR} = \lim_{r'\to\infty} c_{\rm o}(r') = \hat{c}_{IR} = \lim_{r'\to\infty} \hat{c}_{\rm o}(r') = 2\,\frac{k-1}{k+2} . \tag{50}
$$

In summary, collecting the results (49) and (50), we can express equation (39) explicitly in terms of the level k,

$$
c(r, M_{\tilde{c}}^{\tilde{k}}) \approx \begin{cases} 4\,\frac{k-1}{k+2}\,, & \text{for} \quad 1 \ll \frac{2}{r} \ll M_{\tilde{c}}^{\tilde{k}} \\ 6\,\frac{k-1}{k+3}\,, & \text{for} \quad M_{\tilde{c}}^{\tilde{k}} \ll \frac{2}{r} \end{cases} . \tag{51}
$$

We have replaced the limits in (39) by mass scales in order to exhibit the underlying physical picture. Here $M_{\tilde{c}}^{\tilde{k}}$ is the smallest mass of an unstable bound state which may be formed in the process $(a,i) + (b,j) \to (\tilde{c}, \tilde{k})$ for $K_{ij}^{g} \neq 0, 2$. We also used that the Breit-Wigner formula (11) implies that $M_{\tilde{c}}^{\tilde{k}} \sim e^{\sigma/2}$ for large positive σ.

First one should note that in the deep UV limit we obtain the same effective central charge as in section 3.1, albeit in a quite different manner. On the mathematical side this implies some non-trivial identities for Rogers dilogarithm and on the physical (51) exhibits a more detailed behaviour than the analysis in section 3.1. In the first regime the lower limit indicates the onset of the lightest stable soliton in the two copies of complex sine-Gordon model. The unstable particles are on an energy scale much larger than the temperature of the system. Thus, the dynamical interaction between solitons of different colours is "frozen" and we end up with two copies of the $SU(2)_k/U(1)$ coset which do not interact with each other. As soon as the parameter r reaches the energy scale of the unstable solitons with mass $M_{\tilde{c}}^{\tilde{k}}$, the solitons of different colours start to interact, being now enabled to form bound states. This interaction breaks parity and forces the system to approach the $SU(3)_k/U(1)^2$ coset model with central charge given by the formula in (2) for $G = SU(3)$.

The case when σ tends to infinity is special and one needs to pay attention to the order in which the limits are taken, we have

$$4\,\frac{k-1}{k+2} = \lim_{r\to 0}\lim_{\sigma\to\infty} c(r,\sigma) \neq \lim_{\sigma\to\infty}\lim_{r\to 0} c(r,\sigma) = 6\,\frac{k-1}{k+3}\,. \tag{52}$$

One might enforce an additional step in the scaling function by exploiting the fact that the mass ratio m_1/m_2 is not fixed. So it may be chosen to be very large or very small. This amounts to decouple the TBA systems for solitons with different colour by shifting one system to the infrared with respect to the scale parameter r. The plateau then has an approximate width of $\sim \ln|m_1/m_2|$ (see figure 2). However, as soon as r becomes small enough the picture we discussed for $m_1 \sim m_2$ is recovered.

4.3 Restoring parity and eliminating the resonances

In this subsection we are going to investigate the special limit $\sigma \to 0$ which is equivalent to choosing the vector couplings $\Lambda_\pm$ in (1) parallel or anti-parallel. For the classical theory it was pointed out in [5] that only then the equations of motion are parity invariant. Also the TBA-equations become parity invariant in the absence of the resonance shifts, albeit the S-matrix still violates it through the phase factors η. Since in the UV regime a small difference in the masses m_1 and m_2 does not effect the outcome of the analysis, we can restrict ourselves to the special situation $m_1 = m_2$, in which case we obtain two identical copies of the system

$$\epsilon_a(\theta) + \sum_{b=1}^{k-1} (\phi_{ab} + \psi_{ab}) * L_b(\theta) = r\, M_a \cosh\theta\,. \tag{53}$$

Then we have $\epsilon_a(\theta) = \epsilon_a^{(1)}(\theta) = \epsilon_a^{(2)}(\theta)$, $M_a = M_a^{(1)} = M_a^{(2)}$ and the scaling function is given by the expression

$$c(r, \sigma = 0) = \frac{6\,r}{\pi^2} \sum_{a=1}^{k-1} M_a \int d\theta\; L_a(\theta)\cosh\theta\,. \tag{54}$$

The factor two in comparison with (19) takes the two copies for $i = 1, 2$ into account. The discussion of the high-energy limit follows the standard arguments similar to the one of the preceding subsection and as may be found in [2, 29]. Instead of shifting by the resonance parameter σ, one now shifts the TBA equations by $\ln r/2$. The constant TBA equation which determines the UV central charge then just coincides with (41). We therefore obtain

$$\lim_{r\to 0}\lim_{\sigma\to 0} c(r,\sigma) = \frac{12}{\pi^2}\sum_{a=1}^{k-1} L\left(\frac{x_a}{1+x_a}\right) = 6\,\frac{k-1}{k+3}\;. \tag{55}$$

Thus, again we recover the coset central charge (2) for $G = SU(3)$, but this time without breaking parity in the TBA equations. This is in agreement with the results of section 3.1, which showed that we can obtain this limit for any finite value of σ.

4.4 Universal TBA equations and Y-systems

Before we turn to the discussion of specific examples for definite values of the level k, we would like to comment that there exists an alternative formulation of the TBA equations (16) in terms of a single integral kernel. This variant of the TBA equations is of particular advantage when one wants to discuss properties of the model and keep the level k generic. By means of the convolution theorem and the Fourier transforms of the TBA kernels ϕ and ψ, which can be read off directly from (29) and (30), one derives the set of integral equations

$$\epsilon_a^i(\theta) + \Omega_k * L_a^j(\theta - \sigma_{ji}) = \sum_{b=1}^{k-1} I_{ab}\,\Omega_k * (\epsilon_b^i + L_b^i)(\theta)\;. \tag{56}$$

We recall that I denotes the incidence matrix of $su(k)$ and the kernel Ω_k is found to be

$$\Omega_k(\theta) = \frac{k/2}{\cosh(k\theta/2)}\;. \tag{57}$$

The on-shell energies have dropped out because of the crucial relation [31]

$$\sum_{b=1}^{k-1} I_{ab} M_b^i = 2\cos\tfrac{\pi}{k}\, M_a^i\;, \tag{58}$$

which is a property of the mass spectrum inherited from affine Toda field theory. Even though the explicit dependence on the scale parameter has been lost, it is recovered from the asymptotic condition

$$\epsilon_a^i(\theta) \underset{\theta\to\pm\infty}{\longrightarrow} r M_a^i\, e^{\pm\theta}\;. \tag{59}$$

The integral kernel present in (56) has now a very simple form and the k dependence is easily read off.

Closely related to the TBA equations in the form (56) are the following functional relations also referred to as Y-systems. Using complex continuation (see e.g. [14] for a similar computation) and defining the quantity $Y_a^i(\theta) = \exp(-\epsilon_a^i(\theta))$ the integral equations are replaced by

$$Y_a^i(\theta + \tfrac{i\pi}{k})Y_a^i(\theta - \tfrac{i\pi}{k}) = \left[1 + Y_a^j(\theta - \sigma_{ji})\right] \prod_{b=1}^{k-1} \left[1 + Y_b^i(\theta)^{-1}\right]^{-I_{ab}} . \qquad (60)$$

The Y-functions are assumed to be well defined on the whole complex rapidity plane where they give rise to entire functions. These systems are useful in many aspects, for instance they may be exploited in order to establish periodicities in the Y-functions, which in turn can be used to provide approximate analytical solutions of the TBA-equations. The scaling function can be expanded in integer multiples of the period which is directly linked to the dimension of the perturbing operator.

Noting that the asymptotic behaviour of the Y-functions is $\lim_{\theta\to\infty} Y_a^i(\theta) \sim e^{-rM_a^i \cosh\theta}$, we recover for $\sigma \to \infty$ the Y-systems of the $su(k)$-minimal ATFT derived originally in [28]. In this case the Y-systems were shown to have a period related to the dimension of the perturbing operator (see (84)). We found some explicit periods for generic values of the resonance parameter σ as we discuss in the next section for some concrete examples.

5 Explicit examples

In this section we support our analytical discussion with some numerical results and in particular justify various assumptions for which we have no rigorous analytical argument so far. We numerically iterate the TBA-equations (16) and have to choose specific values for the level k for this purpose. As we pointed out in the introduction, quantum integrability has only been established for the choice $k \geq h$. Since the perturbation is relevant also for smaller values of k and in addition the S-matrix makes perfect sense for these values of k, it will be interesting to see whether the TBA-analysis in the case of $su(3)_k$ will exhibit any qualitative differences for $k < 3$ and $k \geq 3$. From our examples for the values $k = 2, 3, 4$ the answer to this question is that there is no apparent difference. For all cases we find the staircase pattern of the scaling function predicted in the preceding section as the values of σ and x sweep through the different regimes. Besides presenting numerical plots we also discuss some peculiarities of the systems at hand. We provide the massless TBA equations (32) with their UV and IR central charges and state the Y-systems together with their periodicities. Finally, we also comment on the classical or weak coupling limit $k \to \infty$.

5.1 The $\mathrm{SU}(3)_2$-HSG model

This is the simplest model for the $su(3)_k$ case, since it contains only the two self-conjugate solitons (1,1) and (1,2). The formation of stable particles via fusing is not possible and the only non-trivial S-matrix elements are those between particles of different colour

$$S_{11}^{11} = S_{11}^{22} = -1, \quad S_{11}^{12}(\theta - \sigma) = -S_{11}^{21}(\theta + \sigma) = \tanh \frac{1}{2}\left(\theta - i\frac{\pi}{2}\right) \,. \qquad (61)$$

Here we have chosen $\eta_{12} = -\eta_{21} = i$. One easily convinces oneself that (61) satisfies indeed (9) and (10). This scattering matrix may be related to various matrices which occurred before in the literature. First of all when performing the limit $\sigma \to \infty$ the scattering involving different colours becomes free and the systems consists of two free fermions leading to the central charge $c = 1$. Taking instead the limit $\sigma \to 0$ the expressions in (61) coincide precisely with a matrix which describes the scattering of massless "Goldstone fermions (Goldstinos)" discussed in [13]. Apart from the factor i, the matrix $S_{11}^{21}(\theta)|_{\sigma=0}$ was also proposed to describe the scattering of a massive particle [33]. Having only one colour available one is not able to set up the usual crossing and unitarity equations and in [33] the authors therefore resorted to the concept of "anti-crossing". As our analysis shows this may be consistently overcome by breaking the parity invariance. The TBA-analysis is summarized as follows

$$\begin{array}{rcl} \text{unstable particle formation} & : & c_{su(3)_2} = \dfrac{6}{5} = c_{UV} + \hat{c}_{UV} = \dfrac{7}{10} + \dfrac{1}{2} \\ \text{no unstable particle formation} & : & 2c_{su(2)_2} = 1 = c_{IR} + \hat{c}_{IR} = \dfrac{1}{2} + \dfrac{1}{2} \,. \end{array}$$

It is interesting to note that the flow from the tricritical Ising to the Ising model which was investigated in [13], emerges as a subsystem in the HSG-model in the form $c_{UV} \to c_{IR}$. This suggests that we could alternatively also view the HSG-system as consisting out of a massive and a massless fermion, where the former is described by (36),(32) and the latter by (37),(33), respectively.

Our numerical investigations of the model match the analytical discussion and justifies various assumptions in retrospect. Figure 1 exhibits various plots of the L-functions in the different regimes. We observe that for $\ln(2/r) < \sigma/2$, $\sigma \neq 0$ the solutions are symmetric in the rapidity variable, since the contribution of the ψ kernels responsible for parity violation is negligible. The solution displayed is just the free fermion L-function, $L^i(\theta) = \ln(1 + e^{-rM^i \cosh\theta})$. Approaching more and more the ultraviolet regime, we observe that the solutions L^i cease to be symmetric signaling the violation of parity invariance. The second plateau is then formed, which will extend beyond $\theta = 0$ for the deep ultraviolet (see figure 1). The staircase pattern of the scaling function is displayed in figure 2 for the different cases discussed in the previous section. We observe always the value 6/5 in the deep ultraviolet regime, but depending on the value of the resonance parameter and the mass ratio it may be reached sooner or later. The plateau at 1 corresponds to the situation when the unstable particles can not be formed yet and we only have two copies of $su(3)_2$ which do not interact. Choosing the mass ratios in the two copies to be very different, we can also "switch them on" individually as the plateau at 1/2 indicates.

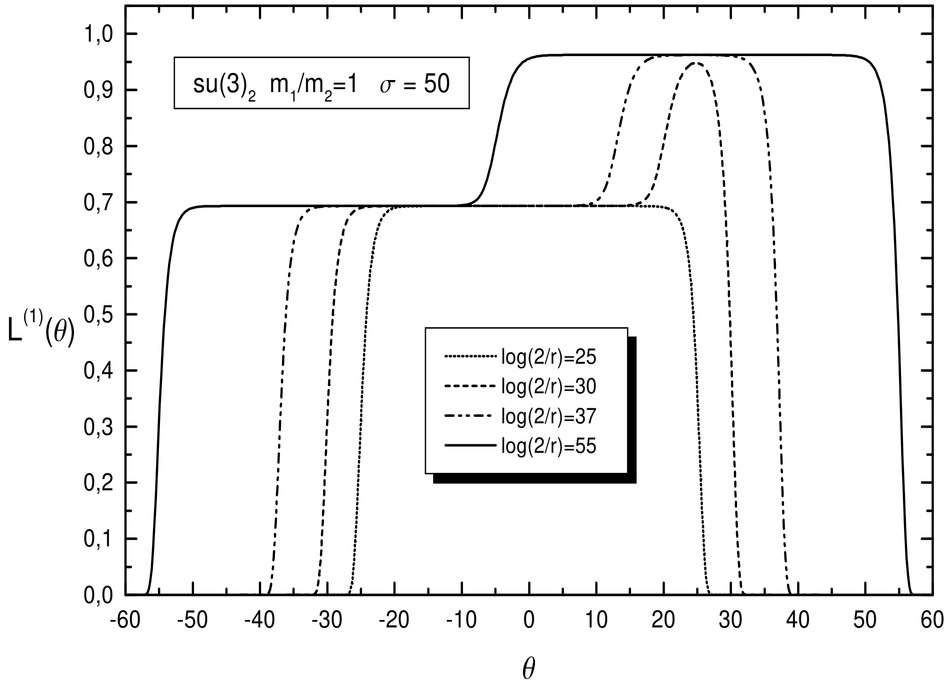

Figure 1: Numerical solution for $L^{(1)}(\theta)$ of the $su(3)_2$ related TBA-equations at different values of the scale parameter r and fixed resonance shift and mass ratio.

The Y-systems (60) for $k = 2$ read

$$Y_1^i\left(\theta + i\frac{\pi}{2}\right) Y_1^i\left(\theta - i\frac{\pi}{2}\right) = 1 + Y_1^j(\theta - \sigma_{ji}) \quad i, j = 1, 2,\ i \neq j\ . \tag{62}$$

For $\sigma = 0$ they coincide with the ones derived in [13] for the "massless" subsystem. Shifting the arguments in (62) appropriately, the periodicity

$$Y_1^i\left(\theta + \frac{5\pi i}{2} + \sigma_{ji}\right) = Y_1^j(\theta) \tag{63}$$

is obtained after few manipulations. For a vanishing resonance parameter (63) coincides with the one obtained in [2, 13]. These periods may be exploited in a series expansion of the scaling function in terms of the conformal dimension of the perturbing operator.

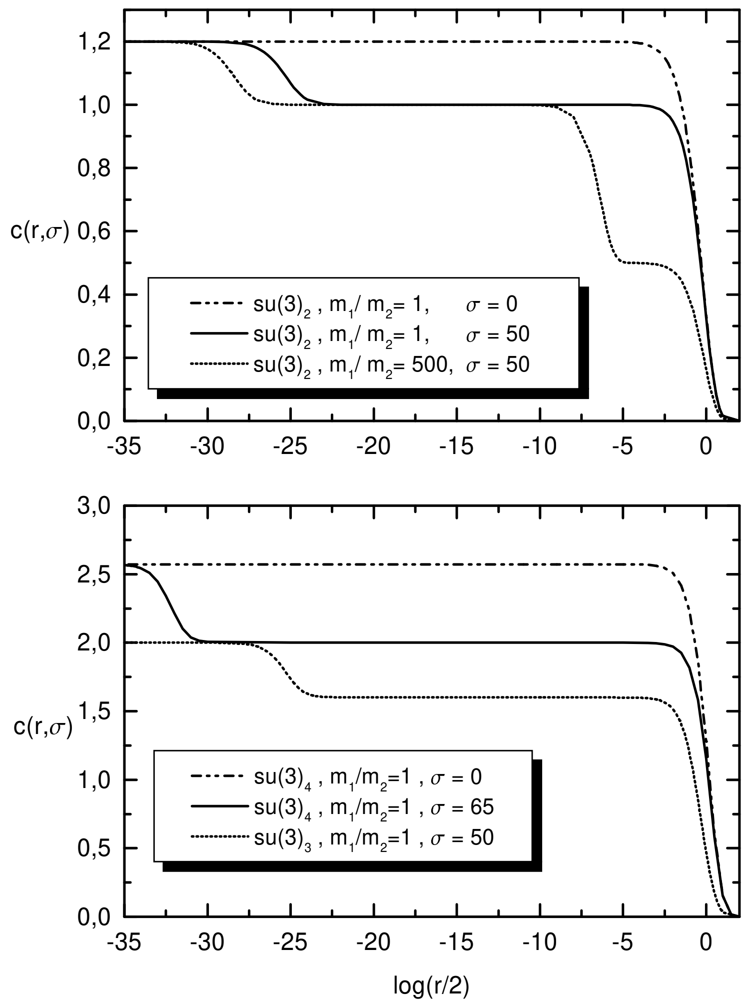

Figure 2: Numerical plots of the scaling function for $su(3)_k$, $k = 2, 3, 4$ as a function of the variable $\log r/2$ at different values of the resonance shift and mass ratio.

5.2 The SU(3)$_3$-HSG model

This model consists of two pairs of solitons $\overline{(1,1)} = (2,1)$ and $\overline{(1,2)} = (2,2)$. When the soliton $(1, i)$ scatters with itself it may form $(2, i)$ for $i = 1, 2$ as a bound state.

The two-particle S-matrix elements read

$$S^{ii}(\theta) = \begin{pmatrix} (2)_\theta & -(1)_\theta \\ -(1)_\theta & (2)_\theta \end{pmatrix} \qquad S^{ij}(\theta - \sigma_{ij}) = \begin{pmatrix} \eta_{ij}\,(-1)_\theta & \eta_{ij}^2\,(-2)_\theta \\ \eta_{ij}^2\,(-2)_\theta & \eta_{ij}\,(-1)_\theta \end{pmatrix} . \quad (64)$$

Since soliton and anti-soliton of the same colour obey the same TBA equations we can exploit charge conjugation symmetry to identify $\epsilon^i(\theta) := \epsilon_1^i(\theta) = \epsilon_2^i(\theta)$ leading to the reduced set of equations

$$\epsilon^i(\theta) + \varphi * L^i(\theta) - \varphi * L^j(\theta - \sigma_{ji}) = rM^i \cosh\theta, \quad \varphi(\theta) = -\frac{4\sqrt{3}\cosh\theta}{1 + 2\cosh 2\theta} . \quad (65)$$

The corresponding scaling function therefore acquires a factor two,

$$c(r,\sigma) = \frac{6\,r}{\pi^2} \sum_i M^i \int d\theta\, \cosh\theta\, L^i(\theta) . \quad (66)$$

This system exhibits remarkable symmetry properties. We consider first the situation $\sigma = 0$ with $m_1 = m_2$ and note that the system becomes free in this case

$$M^{(1)} = M^{(2)} =: M \;\Rightarrow\; \epsilon^{(1)}(\theta) = \epsilon^{(2)}(\theta) = rM\cosh\theta . \quad (67)$$

meaning that the theory falls apart into four free fermions whose central charges add up to the expected coset central charge of 2. Also for unequal masses $m_1 \neq m_2$ the system develops towards the free fermion theory for high energies when the difference becomes negligible. This is also seen numerically.

For $\sigma \neq 0$ the two copies of the minimal A_2-ATFT or equivalently the scaling Potts model start to interact. The outcome of the TBA-analysis in that case is summarized as

$$\begin{aligned} &\text{unstable particle formation} : && c_{su(3)_3} = 2 = c_{UV} + \hat{c}_{UV} = \frac{6}{5} + \frac{4}{5} \\ &\text{no unstable particle formation} : && 2c_{su(2)_3} = \frac{8}{5} = c_{IR} + \hat{c}_{IR} = \frac{4}{5} + \frac{4}{5} . \end{aligned}$$

As discussed in the previous case for $k = 2$ the L-functions develop an additional plateau after passing the point $\ln(2/r) = \sigma/2$. This plateau lies at $\ln 2$ which is the free fermion value signaling that the system contains a free fermion contribution in the UV limit as soon as the interaction between the solitons of different colours becomes relevant. Figure 2 exhibits the same behaviour as the previous case, we clearly observe the plateau at $8/5$ corresponding to the two non-interacting copies of the minimal A_2-ATFT. As soon as the energy scale of the unstable particles is reached the scaling function approaches the correct value of 2.

The Y-systems (60) for $k = 3$ read

$$Y_{1,2}^i\left(\theta + i\frac{\pi}{3}\right) Y_{1,2}^i\left(\theta - i\frac{\pi}{3}\right) = Y_{1,2}^i(\theta)\,\frac{1 + Y_{1,2}^j(\theta + \sigma_{ij})}{1 + Y_{1,2}^i(\theta)} \quad i,j = 1,2,\; i \neq j . \quad (68)$$

Once again we may derive a periodicity

$$Y^i_{1,2}(\theta + 2\pi i + \sigma_{ji}) = Y^j_{1,2}(\theta) \tag{69}$$

by making the suitable shifts in (68) and subsequent iteration.

5.3 The SU(3)$_4$-HSG model

This model involves 6 solitons, two of which are self-conjugate $\overline{(2,1)} = (2,1)$, $\overline{(2,2)} = (2,2)$ and two conjugate pairs $\overline{(1,1)} = (3,1)$, $\overline{(1,2)} = (3,2)$. The corresponding two-particle S-matrix elements are obtained from the general formulae (4) and (6)

$$S^{ii}(\theta) = \begin{pmatrix} (2)_\theta & (3)_\theta(1)_\theta & -(2)_\theta \\ (3)_\theta(1)_\theta & (2)^2_\theta & (3)_\theta(1)_\theta \\ -(2)_\theta & (3)_\theta(1)_\theta & (2)_\theta \end{pmatrix} \tag{70}$$

for soliton-soliton scattering with the same colour values and

$$S^{ij}(\theta - \sigma_{ij}) = \begin{pmatrix} \eta_{ij}(-1)_\theta & \eta^2_{ij}(-2)_\theta & \eta^3_{ij}(-3)_\theta \\ \eta^2_{ij}(-2)_\theta & -(-3)_\theta(-1)_\theta & \eta^2_{ij}(-2)_\theta \\ \eta^3_{ij}(-3)_\theta & \eta^2_{ij}(-2)_\theta & \eta_{ij}(-1)_\theta \end{pmatrix} \tag{71}$$

for the scattering of solitons of different colours with $\eta_{12} = e^{i\frac{\pi}{4}}$. In this case the numerics becomes more involved but for the special case $m_1 = m_2$ one can reduce the set of six coupled integral equations to only two by exploiting the symmetry $L^{(1)}_a(\theta) = L^{(2)}_a(-\theta)$ and using charge conjugation symmetry, $L^i_1(\theta) = L^i_3(\theta)$. The numerical outcomes, shown in figure 2 again match, with the analytic expectations (51) and yield for $\ln(2/r) > \sigma/2$ the coset central charge of 18/7. In summary we obtain

$$\begin{array}{rcl} \text{unstable particle formation} & : & c_{su(3)_4} = \dfrac{18}{7} = c_{UV} + \hat{c}_{UV} = \dfrac{11}{7} + 1 \\ \text{no unstable particle formation} & : & 2c_{su(2)_4} = 2 = c_{IR} + \hat{c}_{IR} = 1 + 1 \ , \end{array}$$

which matches precisely the numerical outcome in figure 2, with the same physical interpretation as already provided in the previous two subsections.

5.4 The semi-classical limit $k \to \infty$

As last example we carry out the limit $k \to \infty$, which is of special physical interest since it may be identified with the weak coupling or equivalently the classical limit, as is seen from the relation $\hbar\beta^2 = 1/k + O(1/k^2)$. To illustrate this equivalence we have temporarily re-introduced Planck's constant. It is clear from the TBA-equations that this limit may not be taken in a straightforward manner. However, we can take it in two steps, first for the on-shell energies and the kernels and finally for the sum over all particle contributions. The on-shell energies are easily computed by noting that the mass spectrum becomes equally spaced for $k \to \infty$

$$M_a^i = M_{k-a}^i = \frac{m_i}{\pi \beta^2} \sin \frac{\pi\, a}{k} \approx a\, m_i \qquad , \quad a < \frac{k}{2} \,. \tag{72}$$

For the TBA-kernels the limit may also be taken easily from their integral representations

$$\phi_{ab}(\theta) \underset{k\to\infty}{\longrightarrow} 2\pi\, \delta(\theta) \left(\delta_{ab} - 2 \left(K_{ab}^{su(k)} \right)^{-1} \right) \quad \text{and} \quad \psi_{ab}(\theta) \underset{k\to\infty}{\longrightarrow} 2\pi\, \delta(\theta) \left(K_{ab}^{su(k)} \right)^{-1} , \tag{73}$$

when employing the usual integral representation of the delta-function. Inserting these quantities into the TBA-equations yields

$$\epsilon_a^i(\theta) \approx r\, a\, m_i \cosh\theta - \sum_{b=1}^{k-1} \left(\delta_{ab} - 2 \left(K_{ab}^{su(k)} \right)^{-1} \right) L_b^i(\theta) - \sum_{b=1}^{k-1} \left(K_{ab}^{su(k)} \right)^{-1} L_b^j(\theta - \sigma) \,. \tag{74}$$

We now have to solve these equations for the pseudo-energies. In principle we could proceed in the same way as in the case for finite k by doing the appropriate shifts in the rapidity. However, we will be content here to discuss the cases $\sigma \to 0$ and $\sigma \to \infty$, which as follows from our previous discussion correspond to the situation of restored parity invariance and two non-interacting copies of the minimal ATFT, respectively. The related constant TBA-equations (42) and (44) become

$$\sigma \to \infty : \; \hat{x}_a \underset{k\to\infty}{\longrightarrow} \frac{(a+1)^2}{a(a+2)} - 1 \quad \text{and} \quad \sigma \to 0 : \; x_a \underset{k\to\infty}{\longrightarrow} \frac{(a+1)(a+2)}{a(a+3)} - 1 \,. \tag{75}$$

The other information we may exploit about the solutions of (74) is that for large rapidities they tend asymptotically to the free solution, meaning that

$$\sigma \to 0, \infty \; : \qquad L_a^i(\theta) \underset{\theta\to\pm\infty}{\longrightarrow} \ln(1 + e^{-r\, a\, m_i \cosh\theta}) \,. \tag{76}$$

We are left with the task to seek functions which interpolate between the properties (75) and (76). Inspired by the analysis in [32] we take these functions to be

$$\sigma \;\to\; \infty \;: \qquad L_a^i(\theta) = \ln \left[\frac{\sinh^2\left(\frac{a+1}{2}\, r m_i \cosh\theta\right)}{\sinh\left(\frac{a}{2}\, r m_i \cosh\theta\right) \sinh\left(\frac{a+2}{2}\, r m_i \cosh\theta\right)} \right] \tag{77}$$

$$\sigma \;\to\; 0 \;: \qquad L_a^i(\theta) = \ln \left[\frac{\sinh\left(\frac{a+1}{2}\, r m_i \cosh\theta\right) \sinh\left(\frac{a+2}{2}\, r m_i \cosh\theta\right)}{\sinh\left(\frac{a}{2}\, r m_i \cosh\theta\right) \sinh\left(\frac{a+3}{2}\, r m_i \cosh\theta\right)} \right] \,. \tag{78}$$

The expression (77) coincides with the expressions discussed in the context of the breather spectrum of the sine-Gordon model [32] and (78) is constructed in analogy. We are now equipped to compute the scaling function in the limit $k \to \infty$

$$c(r,\sigma) = \lim_{k\to\infty} \frac{3\,r}{\pi^2} \sum_{i=1}^{2} \int d\theta\, \cosh\theta \sum_{a=1}^{k-1} M_a^i L_a^i(\theta)\ . \tag{79}$$

Using (72), (77) and (78) the sum over the main quantum number may be computed directly by expanding the logarithm. We obtain for $k \to \infty$

$$c(r)|_{\sigma=\infty} = \frac{-6r}{\pi^2}\sum_{i=1}^{2}\int d\theta\, m_i \cosh\theta \ln\left(1 - e^{-r\, m_i \cosh\theta}\right) \tag{80}$$

$$c(r)|_{\sigma=0} = \frac{-6\,r}{\pi^2}\sum_{i=1}^{2}\int d\theta\ m_i \cosh\theta[\ln\left(1 - e^{-r\, m_i \cosh\theta}\right) + \ln(1 - e^{-r\, 2m_i \cosh\theta})]. \tag{81}$$

Here we have acquired an additional factor of 2, resulting from the identification of particles and anti-particles which is needed when one linearizes the masses in (72). Taking now the limit $r \to 0$ we obtain

$$\text{no unstable particle formation} \quad : \qquad 2\, c_{su(2)_\infty} = 4 \tag{82}$$

$$\text{unstable particle formation} \quad : \qquad c_{su(3)_\infty} = 6\ . \tag{83}$$

The results (80), (82) and (81), (83) allow a nice physical interpretation. We notice that for the case $\sigma \to \infty$ we obtain four times the scaling function of a free boson. This means in the classical limit we obtain twice the contribution of the non-interacting copies of $SU(2)_\infty/U(1)$, whose particle content reduces to two free bosons each of them contributing 1 to the effective central charge which is in agreement with (2). For the case $\sigma \to 0$ we obtain the same contribution, but in addition the one from the unstable particles, which are two free bosons of mass $2m_i$. This is also in agreement with (2).

Finally it is interesting to observe that when taking the resonance poles to be $\theta_R = \sigma - i\pi/k$ the semi-classical limit taken in the Breit-Wigner formula (11) leads to $m_{\tilde{k}}^2 = (m_i + m_j)^2$. On the other hand (81) seems to suggest that $m_{\tilde{k}} = 2m_i$, which implies that the mass scales should be the same. However, since our analysis is mainly based on exploiting the asymptotics we have to be cautious about this conclusion.

6 Conclusions

Our main conclusion is that the TBA-analysis indeed confirms the consistency of the scattering matrix proposed in [4]. In the deep ultraviolet limit we recover the

$G_k/U(1)^\ell$-coset central charge for any value of the $2\ell-1$ free parameters entering the S-matrix, including the choice when the resonance parameters vanish and parity invariance is restored on the level of the TBA-equations. This is in contrast to the properties of the S-matrix, which is still not parity invariant due to the occurrence of the phase factors η, which are required to close the bootstrap equations [4]. However, they do not contribute to our TBA-analysis, which means that so far we can not make any definite statement concerning the necessity of the parity breaking, since the same value for the central charge is recovered irrespective of the value of the σ's. The underlying physical behaviour is, however, quite different as our numerical analysis demonstrates. For vanishing resonance parameter the deep ultraviolet coset central charge is reached straight away, whereas for non-trivial resonance parameter one passes the different regions in the energy scale. Also the choice of different mass scales leads to a theory with a different physical content, but still possessing the same central charge. To settle this issue, it would therefore be highly desirable to carry out the series expansion of the scaling function in r and determine the dimension Δ of the perturbing operator. It will be useful for this to know the periodicities of the Y-functions. We conjecture that they will be

$$Y_a^i\left(\theta+i\pi(1-\Delta)^{-1}+\sigma_{ji}\right)=Y_{\bar{a}}^j(\theta), \qquad (84)$$

which is confirmed by our $su(N)$-examples. For vanishing resonance parameter and the choice $g=su(2)$, this behaviour coincides with the one obtained in [28]. This means the form in (84) is of a very universal nature beyond the models discussed here.

We also observe from our $su(N)$-example that the different regions, i.e. $k\geq h$ and $k<h$, for which quantum integrability was shown and for which not, respectively, do not show up in our analysis.

It would be very interesting to extend the case-by-case analysis of section 5 to other algebras. The first challenge in these cases is to incorporate the different resonance parameters.

Acknowledgments: A.F. and C.K. are grateful to the Deutsche Forschungsgemeinschaft (Sfb288) for financial support and would also like to thank the Departamento de Física de Partículas, Universidad de Santiago de Compostela for kind hospitality. O.A.C. and J.L.M. thank CICYT (AEN99-0589), DGICYT (PB96-0960), and the EC Commission (TMR grant FMRX-CT96-0012) for partial financial support. We are grateful to J. Sánchez Guillén for useful discussions and A. Kuniba for providing informations concerning one of his preprints.

References

[1] C.N. Yang and C.P. Yang, *Phys. Rev.* **147** (1966) 303; *J. Math. Phys.* **10** (1969) 1115.

[2] Al.B. Zamolodchikov, *Nucl. Phys.* **B342** (1990) 695; *Nucl. Phys.* **B358** (1991) 497; *Nucl. Phys.* **B366** (1991) 122.

[3] B. Schroer, T.T. Truong and P. Weisz, *Phys. Lett.* **B63** (1976) 422;

M. Karowski, H.J. Thun, T.T. Truong and P. Weisz, *Phys. Lett.* **B67** (1977) 321;

A.B. Zamolodchikov, *JETP Lett.* **25** (1977) 468.

[4] C.R. Fernández-Pousa and J.L. Miramontes, Integrable QFT with Unstable Particles, hep-th/9910218 (to appear in *Phys. Lett.* **B**).

[5] C.R. Fernández-Pousa, M.V. Gallas, T.J. Hollowood and J.L. Miramontes, *Nucl. Phys.* **B484** (1997) 609.

[6] Q-H. Park, *Phys. Lett.* **B328** (1994) 329;

T.J. Hollowood, J.L. Miramontes and Q-H. Park, *Nucl. Phys.* **B445** (1995) 451.

[7] E. Witten, *Commun. Math. Phys.* **92** (1984) 455;

P. Goddard, A. Kent and D.Olive, *Phys. Lett.* **B152** (1985) 88;

V.A. Fateev and A.B. Zamolodchikov, *Sov. Phys. JETP* **62** (1985) 215;

D. Gepner, *Nucl. Phys.* **B290** (1987) 10;

D. Gepner and Z. Qiu, *Nucl. Phys.* **B285** (1987) 423.

[8] C.R. Fernández-Pousa, M.V. Gallas, T.J. Hollowood and J.L. Miramontes,*Nucl. Phys.* **B499** (1997) 673.

[9] K. Pohlmeyer, *Commun. Math. Phys.* **46** (1976) 207;

F. Lund and T. Regge, *Phys. Rev.* **D14** (1976) 1524;

I. Bakas, *Int. J. Mod. Phys.* **A9** (1994) 3443;

Q-H. Park and H-J. Shin, *Phys. Lett.* **B359** (1995) 125.

[10] A.N. Leznov and M.V. Saveliev, *Commun. Math. Phys.* **89** (1983) 59;

L.A. Ferreira, J.L. Miramontes and J. Sánchez Guillén, *Nucl. Phys.* **B449** (1995) 631.

[11] R. Köberle and J.A. Swieca, *Phys. Lett.* **86B** (1979) 209.

[12] Al.B. Zamolodchikov, Resonance Factorized Scattering and Roaming Trajectories, *Preprint ENS-LPS-335* (1991);

M.J. Martins, Phys. Rev. Lett. **69** (1992) 2461; *Nucl. Phys.* **B394** (1993) 339;

P. Dorey and F. Ravaninni, *Int. J. Mod. Phys.* **A8** (1993) 873; *Nucl. Phys.* **B406** (1993) 708.

[13] Al.B. Zamolodchikov, *Nucl. Phys.* **B358** (1991) 524.

[14] A. Fring, C. Korff and B.J. Schulz, *Nucl. Phys.* **B549** (1999) 579.

[15] A. Fring, C. Korff and B.J. Schulz, On the universal representation of the Scattering matrix of affine Toda field theory, hep-th/9907125 (to appear in *Nucl. Phys.* **B**)

[16] D.I. Olive, *Nuovo Cimento* **26** (1962) 73;

G. Takács and G. Watts, *Nucl. Phys.* **B547** (1999) 538;

J.L. Miramontes, *Phys. Lett.* **455B** (1999) 213.

[17] G. Breit and E.P. Wigner, *Phys. Rev.* **49** (1936) 519;

S. Weinberg, *The Quantum Theory of Fields* (CUP, Cambridge, 1995).

[18] A.E. Arinshtein, V.A. Fateev, and A.B. Zamolodchikov, *Phys. Lett.* **B87** (1979) 389;

H.W. Braden, E. Corrigan, P.E. Dorey and R. Sasaki, *Nucl. Phys.* **B338** (1990) 689.

[19] A.N. Kirillov, *J. Sov. Math.* **47** (1989) 2450.

[20] V.V. Bazhanov and N. Reshetikhin, *J. Phys.* **A23** (1990) 1477;

A. Kuniba, *Nucl. Phys.* **B389** (1993) 209;

A. Kuniba and T. Nakanishi, *Mod. Phys.* **7** (1992) 3487;

A. Kuniba, T. Nakanishi and J. Suzuki, *Mod. Phys.* **8** (1993) 1649; *Int. J. Mod. Phys.* **9** (1994) 5215; *Int. J. Mod. Phys.* **9** (1994) 5267.

[21] E.B. Richmond and G. Szekeres, *J. Austral. Math. Soc.* **A31** (1981) 362;

A. Bytsko and A. Fring, *Nucl. Phys.* **B521** (1998) 573.

[22] A. Bytsko and A. Fring, *Nucl. Phys.* **B532** (1998) 588.

[23] R. Kedem, T.R. Klassen, B.M. McCoy and E. Melzer, *Phys. Lett.* **B304** (1993) 263; *Phys. Lett.* **B307** (1993) 68.

[24] C.R. Fernández-Pousa and J.L. Miramontes, *Nucl. Phys.* **B518** (1998) 745.

[25] K. Pohlmeyer, *Commun. Math. Phys.* **46** (1976) 207;
F. Lund and T. Regge, *Phys. Rev.* **D14** (1976) 1524;
F. Lund, *Phys. Rev. Lett.* **38** (1977) 1175;
B.S. Getmanov, *JETP Lett.* **25** (1977) 119.

[26] A.M. Tsvelik, *Nucl. Phys.* **B305** (1988) 675;
V.A. Fateev, *Int. J. Mod. Phys.* **A6** (1991) 2109;
V.A. Fateev and A.B. Zamolodchikov, *Phys. Lett.* **B271** (1991) 91;
L. Palla, *Phys. Lett.* **B253** (1991) 342;
N. Dorey and T.J. Hollowood, *Nucl. Phys.* **B440** (1995) 215.

[27] Al.B. Zamolodchikov, *Nucl. Phys.* **B358** (1991) 497; *Nucl. Phys.* **B366** (1991) 122.

[28] Al.B. Zamolodchikov, *Phys. Lett.* **B253** (1991) 391.

[29] T.R. Klassen and E. Melzer, *Nucl. Phys.* **B338** (1990) 485; *Nucl. Phys.* **B350** (1991) 635; *Nucl. Phys.* **B370** (1992) 511.

[30] L. Lewin, Dilogarithms and associated functions (Macdonald, London, 1958);
A.N. Kirillov and N. Reshetikhin, *J. Phys.* **A20** (1987) 1587.

[31] M. Freeman, *Phys. Lett.* **B261** (1991) 57;
A. Fring, H.C. Liao and D.I. Olive, *Phys. Lett.* **B266** (1991) 82.

[32] M. Fowler, *Phys. Rev.* **B26** (1985) 2514.

[33] N.Yu. Reshetikhin and F.A. Smirnov, *Commun. Math. Phys.* **131** (1990) 157;
P. Christe and J. Martins, *Mod. Phys. Lett.* **A5** (1990) 2189;
G. Delfino and G. Mussardo, *Phys. Lett.* **B324** (1994) 40.